Chemical Engineering Journal 346 (2018) 1–10

Contents lists available at ScienceDirect

Chemical Engineering Journal

journal homepage: www.elsevier.com/locate/cej

Removal of atorvastatin in water mediated by $CuFe_2O_4$ activated peroxymonosulfate

Dong Miao[a], Jianbiao Peng[a,b], Mengjie Wang[a], Shuai Shao[a], Lianhong Wang[a], Shixiang Gao[a,*]

[a] State Key Laboratory of Pollution Control and Resource Reuse, School of the Environment, Nanjing University, Nanjing 210023, PR China
[b] School of Environment, Henan Normal University, Key Laboratory for Yellow River and Huai River Water Environmental and Pollution Control, Ministry of Education, Henan Key Laboratory for Environmental Pollution Control, Xinxiang, Henan 453007, PR China

HIGHLIGHTS

- Effective removal of ATV from water was achieved by $CuFe_2O_4$/PMS.
- Degradation intermediates were identified and degradation pathways were proposed.
- Intermediate distribution was influenced by the dosage of PMS.
- The main factor affecting the removal of ATV in actual wastewater is organic matter.

GRAPHICAL ABSTRACT

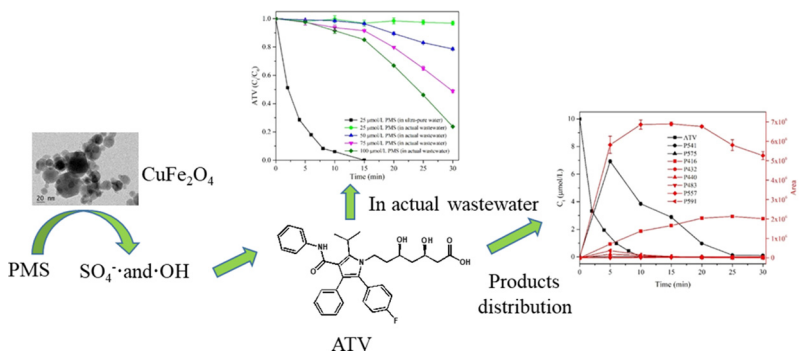

ARTICLE INFO

Keywords:
Atorvastatin
Peroxymonosulfate
$CuFe_2O_4$
Pathways
Intermediate distribution

ABSTRACT

Atorvastatin (ATV) has been widely detected in wastewater treatment plant and aquatic environment. Limited mineralization ratio of ATV in current wastewater treatment processes may result in the accumulation of its transformation intermediates in effluent and cause additional ecological risk to the environment. In this study effectiveness of peroxymonosulfate (PMS) activated by $CuFe_2O_4$ on the degradation of ATV in water were examined. Complete removal of ATV was achieved by using 40 ppm $CuFe_2O_4$ and 25 μ mol dm^{-3} PMS. Eight intermediates were identified and four degradation pathways were proposed. The distribution of major intermediates ATV lactone (P_{541}), hydroxylated ATV lactone (P_{557}) and the pyrrole ring-open intermediate (P_{416}) were monitored with different PMS dosages. As PMS concentration increased from 25 to 150 μ mol dm^{-3}, the main intermediates accumulated were evolved from P_{541} and P_{557} to P_{557} and P_{416}, and all intermediates were completely degraded with 750 μ mol dm^{-3} PMS. 61.72% TOC removal was achieved at pH 7.0 with 100 ppm $CuFe_2O_4$ and 3 m mol dm^{-3} PMS, which indicated that ATV could be well mineralized if PMS and $CuFe_2O_4$ dosages were reasonably used. Overall, this study provided practical knowledge for ATV removal by $CuFe_2O_4$/PMS at ambient temperature.

1. Introduction

Statins are widely used around the world for the treatment of hyperlipidemia by inhibiting the 3-hydroxy-3-methylglutaryl coenzyme A (HMG-CoA) reductase, which is the key enzyme to the production of cholesterol [1,2]. The currently marketed statins include atorvastatin

* Corresponding author.
E-mail address: ecsxg@nju.edu.cn (S. Gao).

https://doi.org/10.1016/j.cej.2018.03.113
Received 15 December 2017; Received in revised form 8 March 2018; Accepted 21 March 2018
Available online 23 March 2018
1385-8947/ © 2018 Elsevier B.V. All rights reserved.

(ATV), simvastatin, fluvastatin, lovastatin, pitavastatin, rosuvastatin and pravastatin [3], in which ATV was the most prescribed one with annual sales of 10 billion dollars worldwide [4]. In 2008, the total retail sales of ATV was 5.88 billion dollars in the United States [5]. Increasing amount of ATV were released into wastewater treatment plant (WWTP) and aquatic environment because of its extensive usage and human excretion [6]. The average concentration of ATV in influent and effluent samples collected from 11 wastewater treatment plants located in Ontario, Canada were 166 and 77 ppt, respectively [7]. The influent concentration of ATV was reported as 1.56 ppb in a medium scale sewage treatment plant located in southeastern USA [8]. Furthermore, the concentration of ATV found in Tennessee River water was 101.3 ppt [9]. Therefore, attention needs to be paid to the potential risk of ATV and its degradation products to aquatic organisms.

Some reports have shown that ATV has certain threat to aquatic organisms. Slightly thicker yolk extension and pericardial edema were observed in zebrafish embryos exposed to 10 μ mol dm^{-3} ATV for 48 h [10]. The numbers of hemorrhagic zebrafish caused by vessel rupture in the head region were increased with increasing ATV concentration when the 6 h post-fertilization zebrafish embryo were exposed to different ATV concentrations (0.05, 0.15, 0.3, 0.5 and 1 μ mol dm^{-3}) for 48 h [11]. In plants, ATV also inhibited the synthesis of sterols. When *L. gibba* was exposed to ATV, the concentration of sterols, which regulated the water permeability of phospholipid bilayer and affected the function of membrane-bound proteins were decreased with the increasing of ATV concentration, and the EC_{50} value was 64 ppb [12]. Although the acute toxicity of ATV to aquatic organisms was negligible at environmentally relevant concentrations, it may have a synergistic effect with other stains in the actual environment. In this sense, it is imperative to develop an effective treatment technique for the removal of ATV and its transformation intermediates in wastewater.

Previous studies have shown that ATV can be removed by indirect photolysis in aqueous solution with long half lifetime (4.89×10^3 s) [13]. It is difficult to completely remove ATV by biodegradation, resulting in the frequent detection of ATV in sludge [5,14]. Advanced oxidation processes (AOPs), such as ozone oxidation, photocatalytic oxidation, Fenton oxidation, has been widely explored in wastewater treatment [15–18]. Sulfate radical ($SO_4^{-}\cdot$)-based AOPs have been recognized as effective alternative method to degrade organic pollutants in wastewater because $SO_4^{-}\cdot$ is more selective and possesses higher mineralization ability towards organic pollutants than hydroxyl radical ($^{\cdot}OH$) [19–21]. $SO_4^{-}\cdot$ can be generated by activation of peroxodisulfate ($S_2O_8^{2-}$, PS) or peroxymonosulfate (HSO_5^{-}, PMS) via heat, UV, transition metals, mixed metal and alkaline [22–27]. Mixed metal catalysts have attracted great interests in activation of PS and PMS because of their polyfunctionality, stability and better catalytic activity [28]. Copper ferrite ($CuFe_2O_4$) has been reported as an effective heterogeneous catalyst in activating persulfates. Zhang et al. have found that $CuFe_2O_4$ showed higher activity and lower Cu^{2+} leaching than CuO at the same dosage [29]. Guan et al. and Jaafarzadeh et al. have reported that atrazine and 2,4-dichlorophenoxyacetic acid could be degraded quickly by using $CuFe_2O_4$ to activate PMS [30,31]. In addition, Ding et al. have found that 10 ppm TBBPA could be completely removed in 30 min by using 100 ppm $CuFe_2O_4$ and 0.2 m mol dm^{-3} PMS [32]. Therefore, $CuFe_2O_4$ was used to activate PMS for the degradation of ATV in this study.

The main purpose of this study is to systematically investigate the oxidative degradation process of ATV by $CuFe_2O_4$/PMS. Firstly, the key factors influencing the transformation of ATV were evaluated including solution pH, PMS concentration and $CuFe_2O_4$ dosage. Secondly, major oxidative species were identified by radical quenching experiment. Thirdly, the identification of transformation intermediates was studied using TOF-LC-MS. Fourthly, the degradation pathways of ATV were proposed, which was verified by the Gaussian theoretical calculations. Then, the distribution of transformation intermediates was analyzed. Finally, the removal efficiency of ATV in actual wastewater was

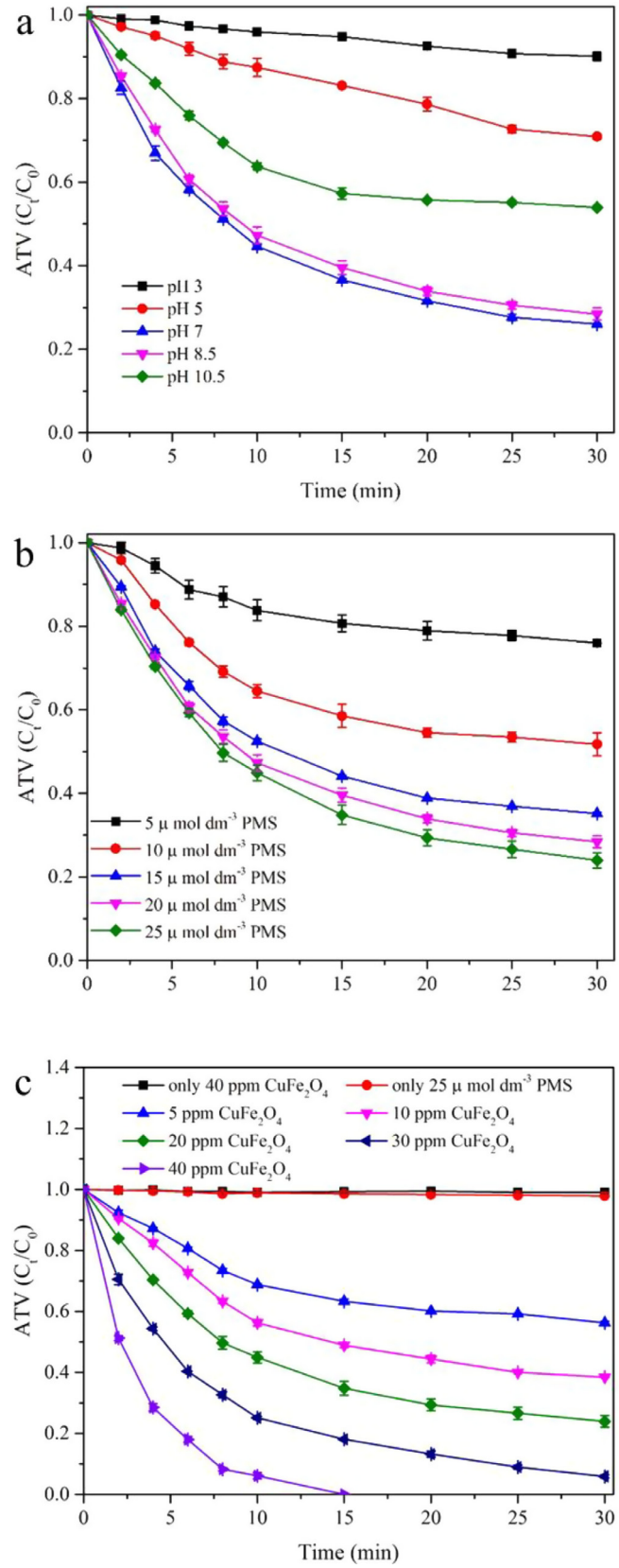

Fig. 1. Effects of (a) initial pH, (b) PMS concentration and (c) $CuFe_2O_4$ dosage on the degradation of ATV. Experimental condition: ATV = 10 μ mol dm^{-3}, T = 25 °C. (a) PMS = 20 μ mol dm^{-3}, $CuFe_2O_4$ = 20 ppm, (b) pH = 7.0, $CuFe_2O_4$ = 20 ppm, (c) pH = 7.0, PMS = 25 μ mol dm^{-3}.

examined.

2. Materials and methods

2.1. Chemicals and reagents

Atorvastatin (ATV, 98.0%) was purchased from J&K Scientific Co. Ltd. Peroxymonosulfate (Oxone, $KHSO_5 \cdot 0.5KHSO_4 \cdot 0.5K_2SO_4$, $KHSO_5 \geq 47\%$), copper iron oxide ($CuFe_2O_4$, 98.5%) and 2,2-azino-bis (3-ethylbenzothiazoline-6-sulfonic acid) ammonium salt (ABTS, 98%) were obtained from Sigma-Aldrich (Shanghai, China). Standards of ATV lactone and 2-hydroxy ATV calcium salt were purchased from Toronto Research Chemicals (Toronto, Canada). HPLC grade methanol was obtained from Tedia Company (Fairfield, USA). Methanol for LC-MS analysis was obtained from Merck Company (Darmstadt, Germany). All of the other reagents were at least of analytical grade or higher. All the stock solutions were prepared by dissolving the chemicals into ultrapure water (18.2 MΩ cm) prepared from a Milli-Q system (Bedford, USA).

2.2. Experimental procedures

The degradation of ATV was performed in a series of headspace vial with PTFE caps at 25 °C, 150 rpm controlled by a thermostatic incubator. The reactor was filled with ATV and PMS solution at predetermined ratios, and subsequently desired amount of $CuFe_2O_4$ was spiked to initiate the reaction. The initial pH of reaction solution was adjusted to desirable values by NaOH (0.1 m mol dm^{-3}) or H_2SO_4 (0.1 m mol dm^{-3}). At designated time intervals, 0.5 mL reaction solution was withdrawn from the reactor, and placed in a centrifuge tube which pre-filled with 0.5 mL methanol to quench the reaction. Then the mixed solution was centrifuged at 10,000 rpm for 10 min, and the residual ATV in the supernatant was determined by high-performance liquid chromatography (HPLC). In the case of actual wastewater, effluents were collected after disinfection at a wastewater treatment plant (WWTP) in Nanjing, China. The effluents were filtrated through 0.22 μm filter and used as the reaction media in comparison tests. All experiments were performed in triplicates and their mean values and standard deviations were reported.

The identification and distribution of ATV degradation intermediates in the reaction process were carried out in a series of 250 mL conical flasks containing 100 mL reaction solution with 40 ppm $CuFe_2O_4$ and three dosage of PMS at 25, 150, and 750 μ mol dm^{-3}. Flasks were collected at different reaction time to obtain a more comprehensive intermediates distribution. The collected reaction solutions were filtered through Teflon filters. Then the filtered reaction solutions were percolated through Oasis HLB SPE cartridges (200 mg, 6 mL, Waters) which were pre-conditioned with 10 mL methanol and 10 mL deionized water at two drops per second. Then, the cartridges were eluted with 2 × 1 mL methanol for the analysis of degradation intermediates by liquid chromatography-tandem mass spectrometry (LC-MS).

2.3. Analytical methods

The residual concentration of ATV was detected by HPLC with a DAD detector. Separation was performed on an Agilent XDB C18 column (5 μm, 4.6 mm × 150 mm, i.d.) at 30 °C. The mobile phase was methanol/water (0.3% formic acid) at a ratio of 70:30 (v/v) with a flow rate of 0.3 mL min^{-1} and the injection volume was 20 μL. The detection wavelengths of ATV was 244 nm, which was determined by DAD detector.

The determination of PMS concentration by ultraviolet spectrophotometer was based on the modified method of Zhang et al. [33]. Briefly, 10 mL 2% dilute H_2SO_4, 0.2 mL 20 m mol dm^{-3} $CoCl_2$, 0.5 mL 20 m mol dm^{-3} ABTS and 1 mL sample were mixed together to react for 4 h. The sulfate radical oxidized ABTS to ABTS+ which has the maximum absorption peak at 734 nm. The residual concentration of PMS was calculated by standard curve as shown in Fig. S1.

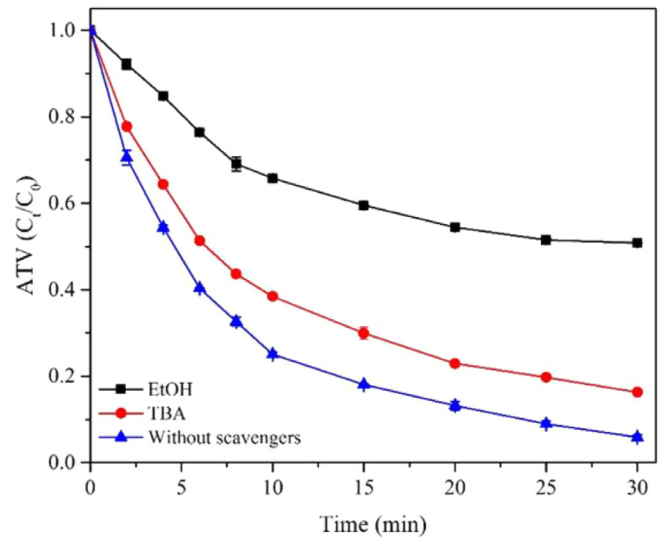

Fig. 2. Effects of ethanol (EtOH) and tert-butanol (TBA) on the degradation of ATV. Experimental condition: ATV = 10 μ mol dm^{-3}, T = 25 °C, pH = 7.0, PMS = 25 μ mol dm^{-3}, $CuFe_2O_4$ = 30 ppm, EtOH = 50 m mol dm^{-3} and TBA = 50 m mol dm^{-3}.

The intermediates generated from ATV degradation were identified by a high-resolution hybrid quadrupole time-of-flight mass spectrometry equipped with a duo-spray ion source (Triple TOF 5600, AB Sciex, Foster City, CA) and an Agilent 1200 series HPLC system. Quantification of ATV lactone and hydroxylated ATV was performed using an Agilent 1200 liquid chromatography coupled with an API 4000 triple quadrupole mass spectrometer (AB Sciex) (LC-MS-MS). Detailed information was shown in Supporting Information (SI) Text S1.

2.4. Calculation of frontier electron density of ATV

The optimized ATV molecular structure parameters were obtained by Gaussian 09 software package with the B3LYP and 6-311G** basis set for molecular orbital calculations. Afterwards, the energy of highest occupied molecular orbital (HOMO) and the lowest unoccupied molecular orbital (LUMO) of all the atoms except hydrogen in ATV molecule were determined to predict the oxidative degradation behavior of ATV.

3. Results and discussion

3.1. Degradation of ATV at different reaction conditions

The effect of initial pH on the degradation of ATV was illustrated in Fig. 1. The removal rate of ATV increased with the increase of pH from acid to neutral and decreased under alkaline condition (Fig. 1a). The removal rate of ATV in 30 min varied from 9.8% to 73.9% at pH range from 3.0 to 10.5 with the highest rate at pH 7 (73.9%). The phenomenon can be explained in the following aspects: $CuFe_2O_4$ nanoparticles are easily dissolved under acidic conditions to release metal ions (shown in Fig. S5a), resulting in greatly reduced activity of the catalyst. Therefore, the removal rate of ATV decreased when pH decreased from 5.0 to 3.0. When the reaction solution was under neutral conditions, the negatively charged ATV ion (pKa (ATV) = 4.33 [34]) and PMS in the form of HSO_5^- (pKa (PMS) = 9.4 [35]) will interact with the positively charged surface of $CuFe_2O_4$ (pH_{pzc} = 7.9 [36]) by electrostatic attraction and speed up the reaction. Hence, the best removal efficiency of ATV was achieved at pH 7.0. On the other hand, when pH was higher

Table 1
Tentative identification of intermediate formed during the oxidative degradation of ATV using TOF-LC-MS.

Compounds	Suggested Structure	RetentionTime (min)	Formula	Calculated mass	Observed mass	Error (ppm)
ATV	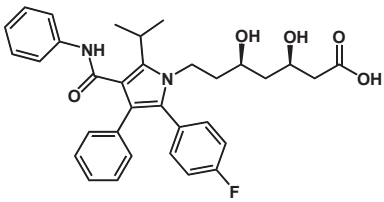	5.244	$C_{33}H_{35}O_5N_2F$	559.2602	559.2568	-6.3
P_{416}	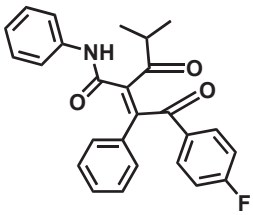	7.273	$C_{26}H_{22}O_3NF$	416.1656	416.1645	-2.8
P_{432}	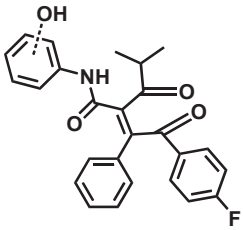	5.939	$C_{26}H_{22}O_4NF$	432.1605	432.1604	-0.4
P_{440}	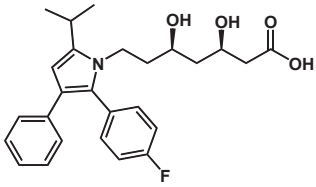	4.295	$C_{26}H_{30}O_4NF$	440.2231	440.2224	-1.5
P_{483}	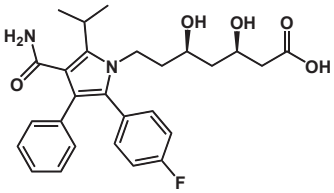	4.105	$C_{27}H_{31}O_5N_2F$	483.2289	483.2280	-1.9
P_{541}	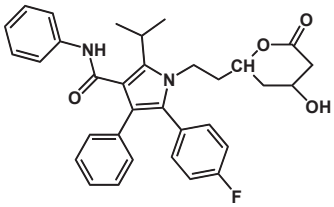	5.634	$C_{33}H_{33}O_4N_2F$	541.2497	541.2521	4.5
P_{557}	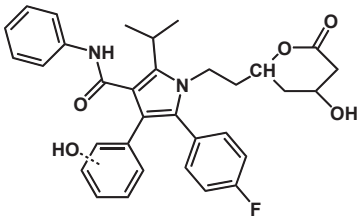	6.230	$C_{33}H_{33}O_5N_2F$	557.2446	557.2479	6.0
P_{575}	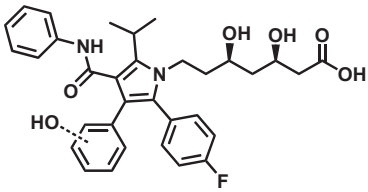	5.359	$C_{33}H_{35}O_6N_2F$	575.2551	575.2565	2.3

(*continued on next page*)

Table 1 (*continued*)

Compounds	Suggested Structure	RetentionTime (min)	Formula	Calculated mass	Observed mass	Error (ppm)
P_{591}	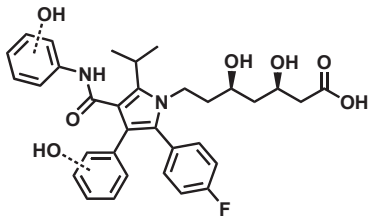	5.288	$C_{33}H_{35}O_7N_2F$	591.2501	591.2520	3.2

Experimental condition: ATV = 10 μ mol dm^{-3}, T = 25 °C, pH = 7.0, PMS = 25–750 μ mol dm^{-3}, $CuFe_2O_4$ = 40 ppm and reaction time = 30 min.

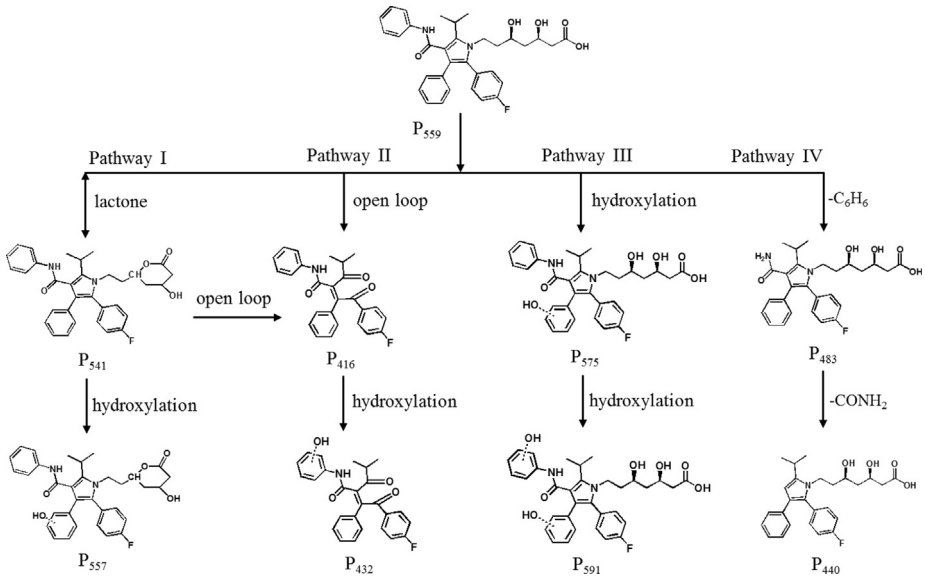

Fig. 3. Proposed degradation pathways for ATV in $CuFe_2O_4$/PMS system.

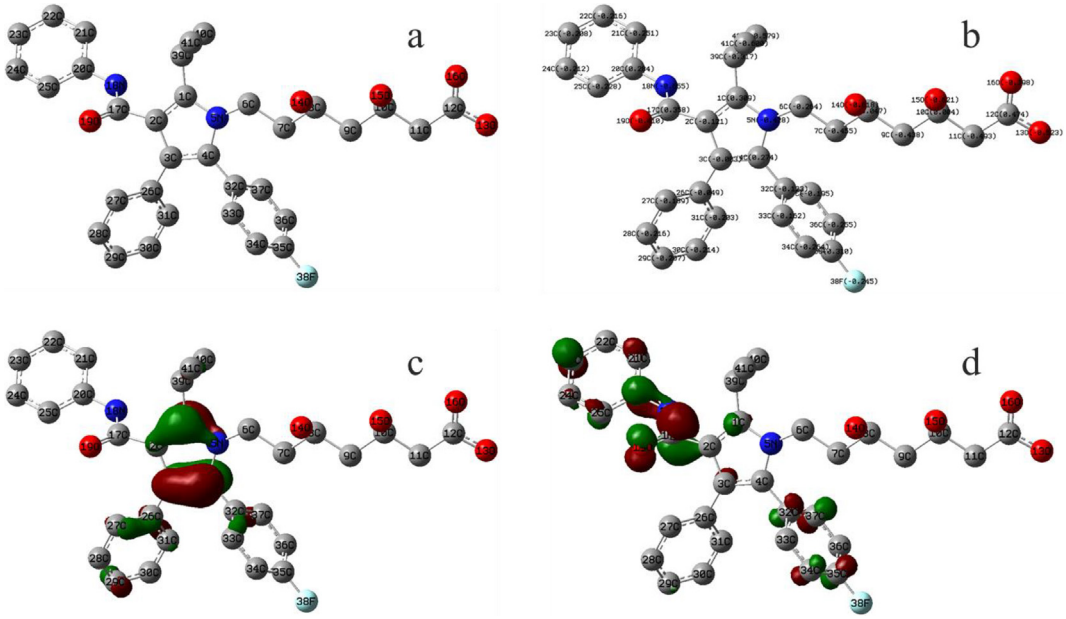

Fig. 4. Mulliken atomic charges and computed FEDs of ATV calculated by Gaussian 09 program at the B3LYP/6-311G* level: (a) The conformation of ATV after optimization, (b) Mulliken atomic charges of ATV, (c) isodensity surfaces of HOMO with an isovalue of 0.05, (d) isodensity surfaces of LUMO with an isovalue of 0.05.

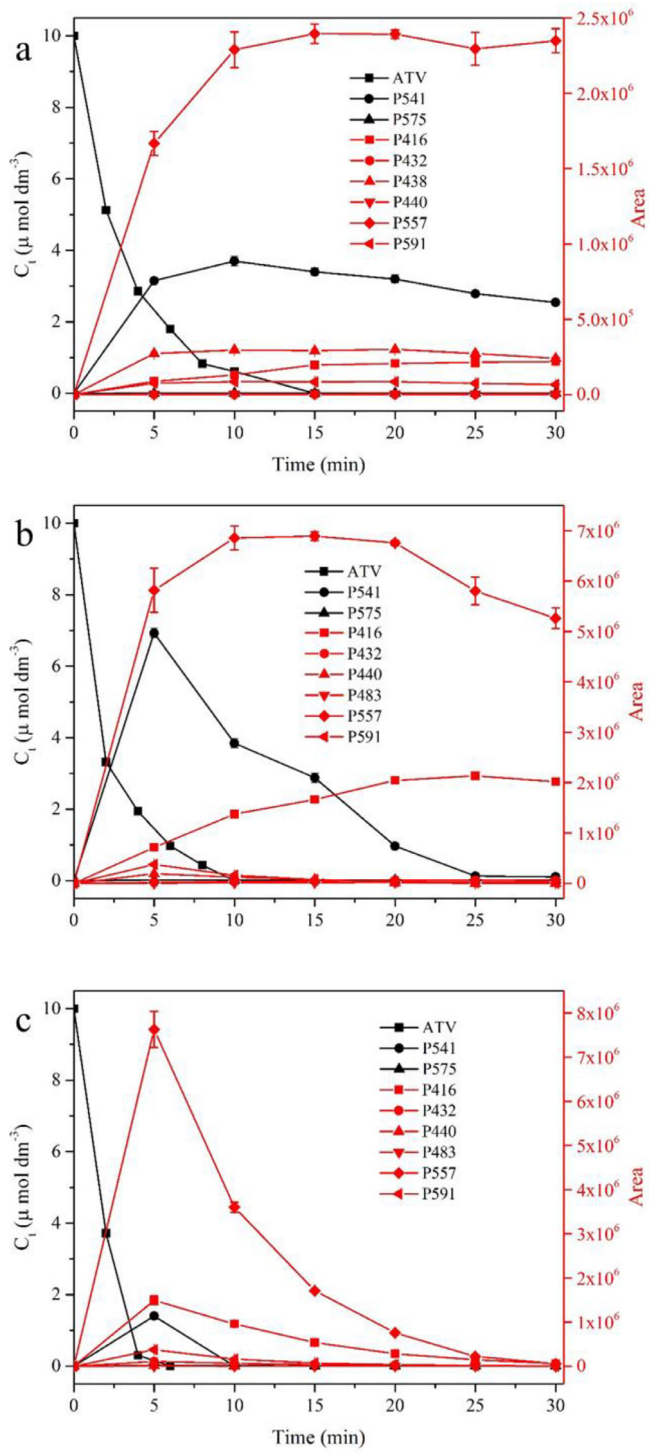

Fig. 5. The distribution of the ATV and its intermediates in $CuFe_2O_4$/PMS system. Experimental condition: ATV = 10 μ mol dm^{-3}, T = 25 °C, pH = 7.0 and $CuFe_2O_4$ = 40 ppm. (a) PMS = 25 μ mol dm^{-3}, (b) PMS = 150 μ mol dm^{-3} and (c) PMS = 750 μ mol dm^{-3}.

than pH_{pzc}, the negative charge on the surface of $CuFe_2O_4$ would form an electrostatic repulsion between the negatively charged PMS (SO_5^{2-}) and dissociated ATV which resulted in the reduced activation efficiency of PMS, and thus reducing the removal rate of ATV.

The effect of initial PMS concentration on the degradation of ATV was presented in Fig. 1b. The removal rate of ATV increased from 24.1% to 76.1% as PMS concentration elevated from 5 to 25 μ mol dm^{-3}. The possible reason was that the more PMS, the more free radicals were produced, leading to higher degradation of ATV. However, when the concentration of PMS was between 15 and 25 μ mol dm^{-3}, the degradation rate of ATV was not significantly increased which may be attributed to the saturation of active sites on the surface of $CuFe_2O_4$, leading to the ineffective activation of excess PMS.

$CuFe_2O_4$ dosage is a critical parameter in contaminant decomposition in $CuFe_2O_4$/PMS system which will control the activation degree of PMS. Fig. 1c showed the degradation of ATV at different $CuFe_2O_4$ dosage with the initial PMS concentration fixed at 25 μ mol dm^{-3}. ATV was completely degraded after 15 min with the $CuFe_2O_4$ dosage of 40 ppm compared with only 43.8% degradation after 30 min when the dosage of $CuFe_2O_4$ was 5 ppm. The results suggested that the degradation of ATV in PMS/$CuFe_2O_4$ system was highly $CuFe_2O_4$ dependent. With the increase of the $CuFe_2O_4$ dosage, the surface active sites also increased, resulting in higher PMS activation rate and higher ATV removal rate. In the case of only $CuFe_2O_4$ or only PMS, no degradation of ATV was observed, which also proved the above results.

3.2. Identification of major oxidative species

Activation of PMS by metal catalysts usually produces $SO_4^{\cdot-}$ and $^{\cdot}OH$ [28]. In order to explore the degradation mechanism of ATV, ethanol (EtOH) and tert-butanol (TBA) were selected as radical scavengers to determine the major radical for ATV oxidation. EtOH can react rapidly with both $SO_4^{\cdot-}$ and $^{\cdot}OH$, and TBA has high reactivity with $^{\cdot}OH$ but poor reactivity with $SO_4^{\cdot-}$ [37]. As exhibited in Fig. 2, when no quencher was added, ATV was degraded by 94.09% in 30 min. In the presence of 50 m mol dm^{-3} TBA, the degradation rate of ATV was reduced to 83.68% in the same reaction time. However, the ATV removal rate was only 49.21% after addition of 50 m mol dm^{-3} EtOH. The result suggested that $SO_4^{\cdot-}$ and $^{\cdot}OH$ were both responsible for the degradation of ATV, and $SO_4^{\cdot-}$ played a more important role.

3.3. Identification of oxidation intermediates and speculation of degradation pathways

The oxidation intermediates of ATV were monitored by TOF-LC-MS with MS^2 scan in the positive mode. Eight intermediates were detected and their proposed structures were listed in Table 1. Structural identification of the intermediates was based on the MS^2 spectra analysis and the comparison with standard substances (Fig. S7).

Based on the identified oxidation intermediates, four degradation pathways of ATV were proposed (Fig. 3). Pathway I: the hydroxyl group and carboxyl group on the ATV branch were dehydrated to produce P_{541}, which was a reversible reaction. P_{541} was then attacked by $^{\cdot}OH$ to generate the hydroxylated product P_{557}. Pathway II: after the tertiary amine in the five-membered pyrrole ring was attacked by $SO_4^{\cdot-}$ and $^{\cdot}OH$, the carbon radicals were formed by the C-N bonds cleavage, which were further oxidized to form P_{416}. Furthermore, the aromatic ring in P_{416} could undergo hydroxylation reaction to produce P_{432}. Pathway III represented the electrophilic addition reaction through $^{\cdot}OH$ attacking on the ATV aromatic ring to produce the hydroxylated product P_{575}, which was further hydroxylated to form P_{591}. Pathway IV: the secondary amine on the ATV was attacked by $SO_4^{\cdot-}$ and $^{\cdot}OH$, resulting in the split of the C-N bond followed by the loss of a phenyl group to form P_{483}. P_{483} was further attacked by $SO_4^{\cdot-}$ and $^{\cdot}OH$ to lose the $-CONH_2$ to form P_{440}.

3.4. Studies of frontier electron densities (FEDs)

Many reports have proved that the frontier electron theory is feasible to predict the oxidative degradation behavior of pollutants [38]. Based on the frontier orbital theory we not only know that atoms with a larger $2FED^2_{HOMO}$ are likely to be electronically extracted, but also know that atoms with higher value of $FED^2_{HOMO} + FED^2_{LOMO}$ are easily attacked by free radicals. In addition, the atoms with more negative

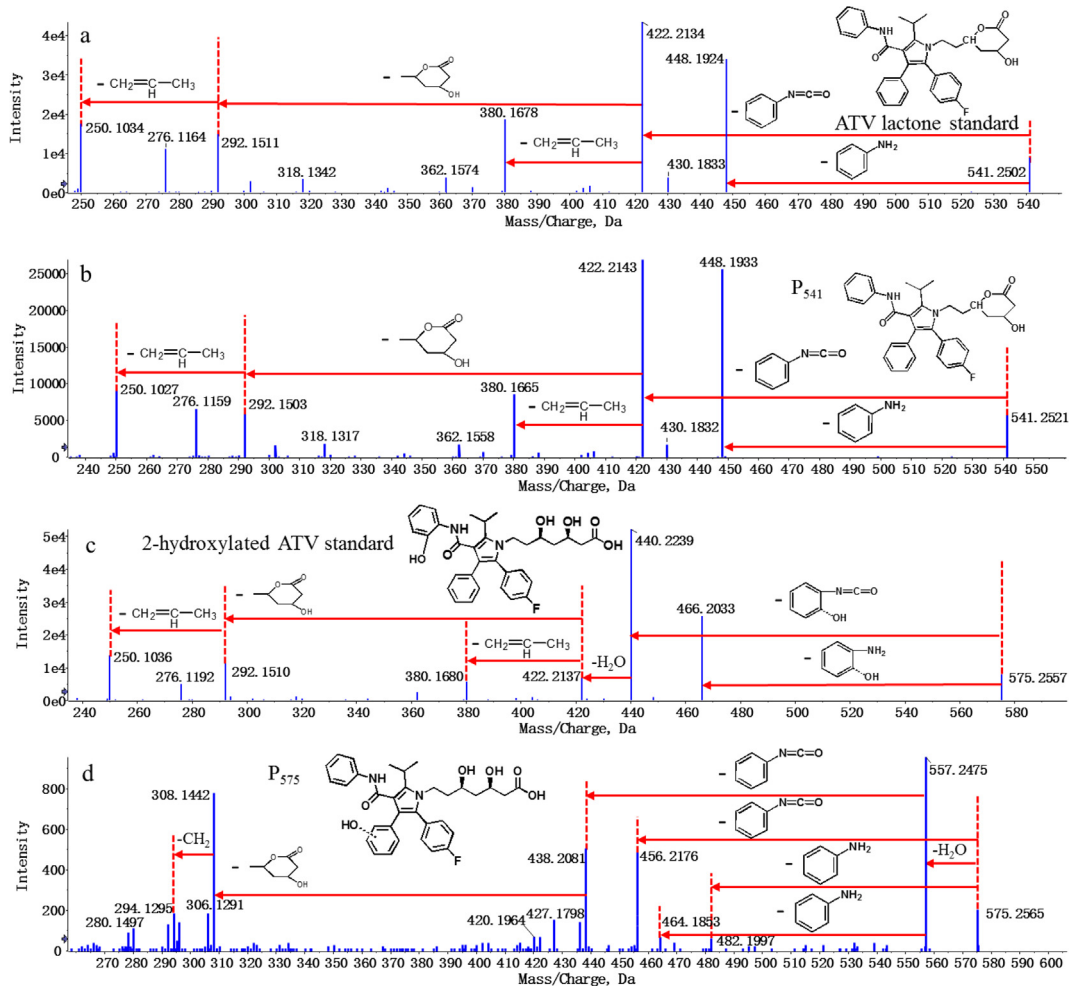

Fig. 6. Transformation intermediates of ATV lactone standard (a), P_{541} (b), 2-hydroxylated ATV standard (c) and P_{575} (d) obtained by TOF-MS/MS and proposed fragmentation pathway.

Table 2
Composition and properties of wastewater sample collected from disinfection effluent

Water type	Coordinate	Alkalinity (as $CaCO_3$, mg/L	pH	TOC (mg/L)	NO_3^- (mmol/L)	SO_4^{2-} (mmol/L)	Cl^- (mmol/L)
Disinfection effluents	118.748088°E 32.249744°N	5.18	7.29	3.96	4.53	2.93	6.40

charges are prone to oxidation reaction [39]. The conformation of ATV after optimization, the Mulliken atomic charges, the isosurface of the HOMO and the isosurface of the LUMO were displayed in Fig. 4. As shown in Fig. 4b, the nitrogen (N(18)) in the secondary amine group possessed the most negative Mulliken atomic charge, followed by the oxygen in the hydroxyl group (O(15) and O(14)). Thus, the nitrogen and two oxygen atoms would be easily oxidized (Pathway I). In addition, the atoms with higher $2FED^2_{HOMO}$ value in the ATV molecule were C(4), followed by C(1) and C(3) (Tab. S1), which suggested that the cleavages of the two bonds between C(1)–N(5) and C(4)–N(5) were reasonable (Pathway II). The HOMO isosurface in Fig. 4c was consistent with this conclusion. The atoms with higher $FED^2_{HOMO} + FED^2_{LOMO}$ value in the ATV molecule were C(17), followed by C(1), C(4), C(3) and C(20) (Table S1), which indicated that C(17) was most likely to be attacked by $SO_4^{\cdot-}$ and $^{\cdot}OH$ (Pathway IV) and the hydroxylated products were generated by ·OH attack on C(20) (Pathway III). The LUMO isosurface shown in Fig. 4d also supported this conclusion.

3.5. Distribution of oxidation intermediates

PMS concentration influenced the distribution of the degradation intermediates in $CuFe_2O_4$/PMS system. To better understand the effect of PMS dosage on the intermediates distribution, we examined the changes of eight intermediates in three different PMS concentration systems. From Fig. 5 we can see that P_{541} (ATV lactone), P_{557} (hydroxylated ATV lactone) and P_{416} (the pyrrole ring-open intermediate) are the main intermediates in three different PMS concentration systems.

From Fig. 5a, we could see that initial concentration of 10 μ mol dm^{-3} ATV was degraded to only 0.6 μ mol dm^{-3} after 10 min, and 37% ATV was converted to its lactone form (3.7 μ mol dm^{-3}) when the PMS concentration was 25 μ mol dm^{-3}. After that P_{541} began to decrease slowly. As the PMS concentration increased to 150 μ mol dm^{-3}, 69% ATV was converted to ATV lactone (6.9 μ mol dm^{-3}) in the first 5 min and then P_{541} began to drop until complete removal, which indicated that ATV was first converted to the lactone form at a certain degree of oxidation. In addition, P_{541} only

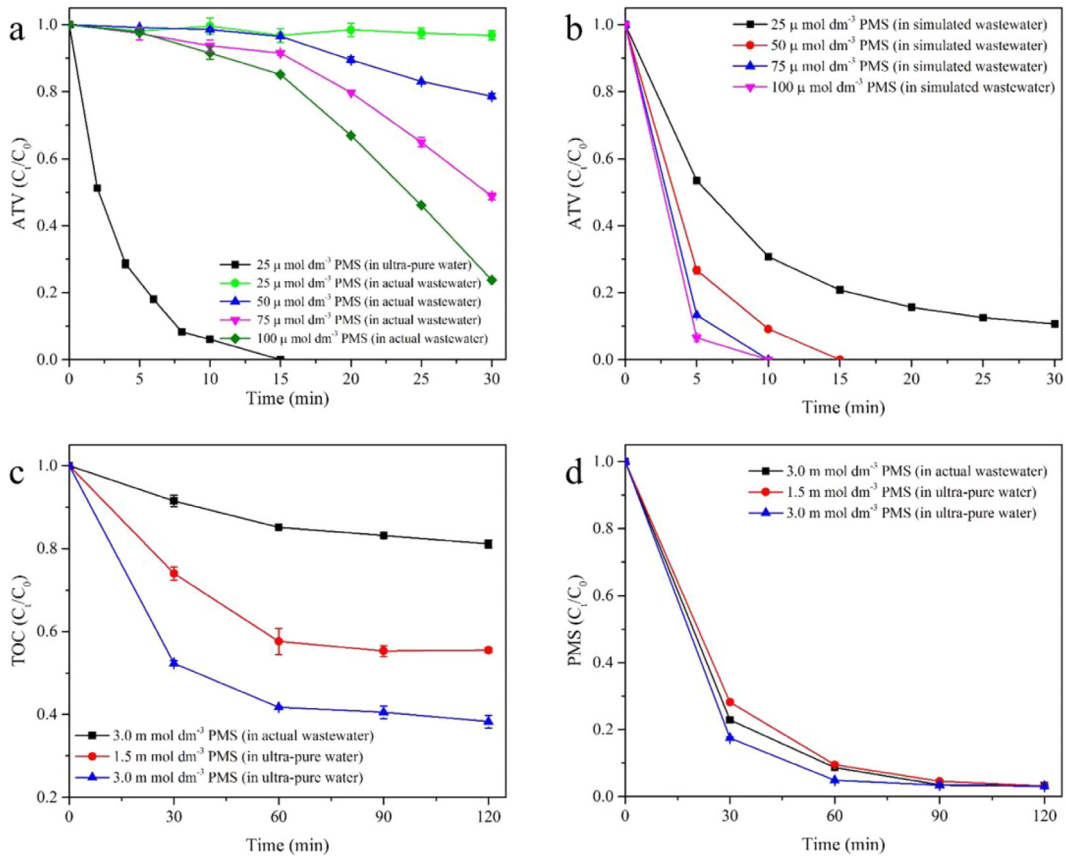

Fig. 7. The degradation of ATV in (a) ultra-pure water and actual wastewater and (b) simulated wastewater. The (c) TOC removal rate and (d) PMS consumption rate in the ultra-pure water and actual wastewater. Experimental condition: ATV = 10 μ mol dm^{-3}, T = 25 °C, pH = 7.29. $CuFe_2O_4$ = 40 ppm for (a) and (b), $CuFe_2O_4$ = 100 ppm for (c) and (d). NO_3^- = 4.53 m mol dm^{-3}, SO_4^{2-} = 2.93 m mol dm^{-3}, Cl^- = 6.40 m mol dm^{-3} and no other organic matter except ATV in simulated wastewater.

accumulated to 1.4 μ mol dm^{-3} in the first 5 min and completely degraded in 10 min at a PMS concentration of 750 μ mol dm^{-3}, indicating that P_{541} was also readily degraded when the concentration of oxidant was high.

P_{557} was the hydroxylation product of P_{541} and deserved special attention. P_{557} gradually accumulated in the first 10 min and remained essentially unchanged afterwards when the PMS concentration was 25 μ mol dm^{-3}. As the concentration of PMS increased to 150 μ mol dm^{-3}, P_{557} began to accumulate in the first 10 min, and remained unchanged after that, which was consistent with the above results. When the PMS concentration was 750 μ mol dm^{-3}, P_{557} was the most cumulative intermediate after 5 min. As the reaction was progressing, P_{557} began to decline rapidly, which indicated that P_{557} was more stable than P_{541}.

P_{416} is a pyrrole ring-open intermediate of ATV and its presence meant that smaller intermediates were produced. At a PMS concentration of 25 μ mol dm^{-3}, the production of P_{416} was very low. However, as the concentration of PMS increased to 150 μ mol dm^{-3}, P_{416} started to accumulate rapidly. When PMS concentration reached 750 μ mol dm^{-3}, P_{416} began to accumulate in the first 5 min and after that it started to degrade slowly. This means that when the oxidant reached a certain concentration, the pyrrole ring of ATV could be opened to produce smaller intermediates.

It has been reported that after oral administration, ATV was mainly metabolized to ATV lactone and two hydroxylated intermediates in humans [40]. We compared the second-order mass spectra of P_{541} generated during the reaction with the ATV lactone standard and found that the spectra were completely consistent (Fig. 6a and b), which indicated that the reaction process indeed generated ATV lactone. As it has been reported that ATV presented in the form of lactone was more cytotoxic than the acid form [1], the conversion of ATV into lactone under low oxidation condition in the natural environment may increase the ecological risk of ATV which needs to be further studied. Unfortunately, we found that the secondary mass spectra of the hydroxylated intermediates P_{575} were not consistent with the 2-hydroxylated ATV standard (Fig. 6c and d). Therefore, we hypothesized that the substitution site of hydroxyl group was likely to be in the fluorine-containing benzene ring or its adjacent benzene ring. Furthermore, the hydroxylation intermediate P_{575} was not a major intermediate in PMS/$CuFe_2O_4$ system. The distribution of other intermediates was shown in Fig. S8.

3.6. Degradation of ATV in actual wastewater and environmental significance of the study

Composition and properties of wastewater sample collected from disinfection effluent of a WWTP were given in Table 2. Inorganic ions (Cl^-, SO_4^{2-}, and NO_3^-) might affect the degradation of ATV because they can be oxidized by $SO_4^-\cdot$ to produce much less reactive radicals [27]. In addition, natural organic matter could compete with ATV for free radicals [37,41]. As indicated in Fig. 7a, the degradation of ATV in actual wastewater was suppressed to a certain extent compared to the reaction in ultra-pure water, mainly due to the presence of organic matter and inorganic ions. In the first 15 min, the degradation of ATV was very slow, probably because the free radicals were consumed by organic matter and inorganic ions in actual wastewater. However, with the increase of PMS concentration, the degradation efficiency of ATV increased gradually. When the PMS concentration was 100 μ mol dm^{-3}, ATV was degraded by 76.3% in 30 min, indicating that ATV was also well removed in actual wastewater. In order to explore the role of

inorganic ions and organic matter on the inhibition of ATV degradation in the actual wastewater, we prepared the simulated wastewater (TOC (2.66 ppm) including ATV and ultra-pure water) according to the inorganic ions concentration in the actual wastewater. The results shown in Fig. 7b indicated that limited inhibitory effect were observed with inorganic ions, which implied that the main reason for the decreased ATV degradation was the existence of organic matter in the actual wastewater which could compete with ATV for free radicals.

In order to better understand the degradation of ATV in $CuFe_2O_4$/PMS system, the mineralization rate of ATV and the consumption of PMS were studied. In theory, 75 mol PMS are needed to totally mineralize 1 mol ATV to CO_2 and H_2O (Eq. (1)). The TOC removal rate with different ATV to PMS ratio was shown in Fig. 7c. When the molar ratio of ATV and PMS were 1:150 and 1:300, TOC was removed by 44.48% and 61.72% in ultra-pure water, which indicated that higher PMS would lead to higher TOC removal. In actual wastewater, the TOC including ATV and organic matter was only removed by 18.9%, when the molar ratio of ATV and PMS was 1:300. This result indicated that the organic matter in actual wastewater consumed a lot of free radicals, and decreased the TOC removal rate. It was worth noting that PMS was almost consumed in the ultra-pure water and actual wastewater (Fig. 7d).

$$C_{33}H_{35}FN_2O_5 + 75\ HSO_5^- \rightarrow 33\ CO_2 + 14\ H_2O + 2\ NH_4^+ + 75\ SO_4^{2-} + F^- + 74\ H^+ \quad (1)$$

In arid and semi-arid areas, re-use of treated municipal wastewater is considered an important way to save water resources. Unfortunately, ATV has been detected in many municipal WWTPs which have no appropriate treatment procedure to remove ATV. Therefore, effective removal of ATV is very important before reusing the wastewater to avoid groundwater pollution. In this case, the $CuFe_2O_4$/PMS system could be an effective way to remove ATV and similar pharmaceuticals because of its polyfunctionality, stability and better catalytic activity.

This study showed the effects of key factors on the ATV degradation in ultrapure water and actual wastewater in $CuFe_2O_4$/PMS oxidation process. In addition, we have also studied the distribution of ATV intermediates at different levels of oxidant, which can predict the accumulation of main intermediates in actual wastewater treatment process.

4. Conclusion

Effective removal of ATV from water was achieved by $CuFe_2O_4$/PMS. The results revealed that increasing the PMS concentration and $CuFe_2O_4$ dosage enhanced the degradation efficiency. Optimized removal of ATV was achieved under neutral condition, which was determined by pKa of ATV, species of PMS, and pH_{pzc} of $CuFe_2O_4$. Four degradation pathways were proposed by the structural analysis of intermediates and the studies of frontier electron densities. The distribution of ATV intermediates at different levels of oxidant could predict the accumulation of main intermediates. The degradation of ATV in wastewater is mainly influenced by organic matter rather than inorganic ions. It is worth noting that toxicological tests are needed to thoroughly assess the toxic effects of the transformation products before this technology could be used in real application.

Acknowledgments

The authors are very grateful for the financial support from the Commonwealth and Environmental protection project for the MEP grant (201509053) and the National Natural Science Foundation of China (No. 21577059).

Appendix A. Supplementary data

Supplementary data associated with this article can be found, in the online version, at http://dx.doi.org/10.1016/j.cej.2018.03.113.

References

[1] K.S. Ellesat, K.-E. Tollefsen, A. Asberg, K.V. Thomas, K. Hylland, Cytotoxicity of atorvastatin and simvastatin on primary rainbow trout (Oncorhynchus mykiss) hepatocytes, Toxicol. In Vitro 24 (2010) 1610–1618.
[2] S. Shao, M. Xu, J. Zhou, X. Ge, G. Chen, L. Guo, L. Luo, K. Li, Z. Zhu, F. Zhang, Atorvastatin attenuates ischemia/reperfusion-induced hippocampal neurons injury via Akt-nNOS-JNK signaling pathway, Cell. Mol. Neurobiol. 37 (2017) 753–762.
[3] T.C. Machado, T.M. Pizzolato, A. Arenzon, J. Segalin, M.A. Lansarin, Photocatalytic degradation of rosuvastatin: Analytical studies and toxicity evaluations, Sci. Total Environ. 502 (2015) 571–577.
[4] Y. Luo, Y. Chen, H. Ma, Z. Tian, Y. Zhang, J. Zhang, Enhancing the biocatalytic manufacture of the key intermediate of atorvastatin by focused directed evolution of halohydrin dehalogenase, Sci. Rep. 7 (2017) 42064.
[5] H.-B. Lee, T.E. Peart, M.L. Svoboda, S. Backus, Occurrence and fate of rosuvastatin, rosuvastatin lactone, and atorvastatin in Canadian sewage and surface water samples, Chemosphere 77 (2009) 1285–1291.
[6] E. Gracia-Lor, J.V. Sancho, R. Serrano, F. Hernandez, Occurrence and removal of pharmaceuticals in wastewater treatment plants at the Spanish Mediterranean area of Valencia, Chemosphere 87 (2012) 453–462.
[7] M.M. Santos, R. Ruivo, M. Lopes-Marques, T. Torres, C.B. de los Santos, L.F.C. Castro, T. Neuparth, Statins: an undesirable class of aquatic contaminants? Aquat. Toxicol. 174 (2016) 1–9.
[8] K.J. Ottmar, L.M. Colosi, J.A. Smith, Sorption of statin pharmaceuticals to wastewater-treatment biosolids, terrestrial soils, and freshwater sediment, J. Environ. Eng-Asce 136 (2010) 256–264.
[9] J.M. Conley, S.J. Symes, S.A. Kindelberger, S.A. Richards, Rapid liquid chromatography-tandem mass spectrometry method for the determination of a broad mixture of pharmaceuticals in surface water, J. Chromatogr. A 1185 (2008) 206–215.
[10] L. D'Amico, I.C. Scott, B. Jungblut, D.Y.R. Stainier, A mutation in zebrafish hmgcr1b reveals a role for isoprenoids in vertebrate heart-tube formation, Curr. Biol. 17 (2007) 252–259.
[11] E. Gjini, L.H. Hekking, A. Kuechler, P. Saharinen, E. Wienholds, J.-A. Post, K. Alitalo, S. Schulte-Merker, Zebrafish Tie-2 shares a redundant role with Tie-1 in heart development and regulates vessel integrity, Dis. Models Mech. 4 (2011) 57–66.
[12] R.A. Brain, T.S. Reitsma, L.I. Lissemore, K. Bestari, P.K. Sibley, K.R. Solomon, Herbicidal effects of statin pharmaceuticals in Lemna gibba, Environ. Sci. Technol. 40 (2006) 5116–5123.
[13] B. Razavi, S. Ben Abdelmelek, W. Song, K.E. O'Shea, W.J. Cooper, Photochemical fate of atorvastatin (lipitor) in simulated natural waters, Water Res. 45 (2011) 625–631.
[14] M.W. Lam, C.J. Young, R.A. Brain, D.J. Johnson, M.A. Hanson, C.J. Wilson, S.M. Richards, K.R. Solomon, S.A. Mabury, Aquatic persistence of eight pharmaceuticals in a microcosm study, Environ. Toxicol. Chem. 23 (2004) 1431–1440.
[15] A. Cruz-Alcalde, C. Sans, S. Esplugas, Priority pesticides abatement by advanced water technologies: The case of acetamiprid removal by ozonation, Sci. Total Environ. 599 (2017) 1454–1461.
[16] J. Peng, H. Shi, J. Li, L. Wang, Z. Wang, S. Gao, Bicarbonate enhanced removal of triclosan by copper(II) catalyzed Fenton-like reaction in aqueous solution, Chem. Eng. J. 306 (2016) 484–491.
[17] J. Peng, J. Xue, J. Li, Z. Du, Z. Wang, S. Gao, Catalytic effect of low concentration carboxylated multi-walled carbon nanotubes on the oxidation of disinfectants with Cl-substituted structure by a Fenton-like system, Chem. Eng. J. 321 (2017) 325–334.
[18] M.J. Sampaio, M.J. Lima, D.L. Baptista, A.M.T. Silva, C.G. Silva, J.L. Faria, Ag-loaded ZnO materials for photocatalytic water treatment, Chem. Eng. J. 318 (2017) 95–102.
[19] J. Deng, Y. Shao, N. Gao, Y. Deng, S. Zhou, X. Hu, Thermally activated persulfate (TAP) oxidation of antiepileptic drug carbamazepine in water, Chem. Eng. J. 228 (2013) 765–771.
[20] P. Hu, M. Long, Cobalt-catalyzed sulfate radical-based advanced oxidation: A review on heterogeneous catalysts and applications, Appl. Catal. B-Environ. 181 (2016) 103–117.
[21] C. Jiang, Y. Ji, Y. Shi, J. Chen, T. Cai, Sulfate radical-based oxidation of fluoroquinolone antibiotics: Kinetics, mechanisms and effects of natural water matrices, Water Res. 106 (2016) 507–517.
[22] X. Du, Y. Zhang, I. Hussain, S. Huang, W. Huang, Insight into reactive oxygen species in persulfate activation with copper oxide: Activated persulfate and trace radicals, Chem. Eng. J. 313 (2017) 1023–1032.
[23] Y. Feng, J. Liu, D. Wu, Z. Zhou, Y. Deng, T. Zhang, K. Shih, Efficient degradation of sulfamethazine with $CuCo_2O_4$ spinel nanocatalysts for peroxymonosulfate activation, Chemi. Eng. J. 280 (2015) 514–524.
[24] J. Liu, Q. Yang, D. Wang, X. Li, Y. Zhong, X. Li, Y. Deng, L. Wang, K. Yi, G. Zeng, Enhanced dewaterability of waste activated sludge by Fe(II)-activated peroxymonosulfate oxidation, Bioresour. Technol. 206 (2016) 134–140.
[25] X. Lou, C. Fang, Z. Geng, Y. Jin, D. Xiao, Z. Wang, J. Liu, Y. Guo, Significantly enhanced base activation of peroxymonosulfate by polyphosphates: Kinetics and mechanism, Chemosphere 173 (2017) 529–534.
[26] N. Zrinyi, A.L. Pham, Oxidation of benzoic acid by heat-activated persulfate: effect of temperature on transformation pathway and product distribution, Water Res. 120 (2017) 43–51.
[27] Y. Xiao, L. Zhang, W. Zhang, K.Y. Lim, R.D. Webster, T.T. Lim, Comparative

evaluation of iodoacids removal by UV/persulfate and UV/H2O2 processes, Water Res. 102 (2016) 629–639.
[28] Y. Du, W. Ma, P. Liu, B. Zou, J. Ma, Magnetic $CoFe_2O_4$ nanoparticles supported on titanate nanotubes ($CoFe_2O_4$/TNTs) as a novel heterogeneous catalyst for peroxymonosulfate activation and degradation of organic pollutants, J. Hazard. Mater. 308 (2016) 58–66.
[29] T. Zhang, H. Zhu, J.-P. Croue, Production of sulfate radical from peroxymonosulfate induced by a magnetically separable $CuFe_2O_4$ spinel in water: efficiency, stability, and mechanism, Environ. Sci. Technol. 47 (2013) 2784–2791.
[30] Y.-H. Guan, J. Ma, Y.-M. Ren, Y.-L. Liu, J.-Y. Xiao, L.-Q. Lin, C. Zhang, Efficient degradation of atrazine by magnetic porous copper ferrite catalyzed peroxymonosulfate oxidation via the formation of hydroxyl and sulfate radicals, Water Res. 47 (2013) 5431–5438.
[31] N. Jaafarzadeh, F. Ghanbari, M. Ahmadi, Efficient degradation of 2,4-dichlorophenoxyacetic acid by peroxymonosulfate/magnetic copper ferrite nanoparticles/ozone: a novel combination of advanced oxidation processes, Chem. Eng. J. 320 (2017) 436–447.
[32] Y. Ding, L. Zhu, N. Wang, H. Tang, Sulfate radicals induced degradation of tetrabromobisphenol A with nanoscaled magnetic $CuFe_2O_4$ as a heterogeneous catalyst of peroxymonosulfate, Appl. Catal. B-Environ. 129 (2013) 153–162.
[33] T. Zhang, Y. Chen, T. Leiknes, Oxidation of refractory benzothiazoles with PMS/$CuFe_2O_4$: kinetics and transformation intermediates, Environ. Sci. Technol. 50 (2016) 5864–5873.
[34] S. Barisci, O. Turkay, The performance of electrosynthesised ferrate (VI) ion, electrocoagulation and peroxi-electrocoagulation processes for degradation of cholesterol-lowering drug atorvastatin, Desalin. Water Treat. 57 (2016) 25561–25571.
[35] C. Tan, N. Gao, Y. Deng, J. Deng, S. Zhou, J. Li, X. Xin, Radical induced degradation of acetaminophen with Fe_3O_4 magnetic nanoparticles as heterogeneous activator of peroxymonosulfate, J. Hazard. Mater. 276 (2014) 452–460.
[36] J. Li, Y. Ren, F. Ji, B. Lai, Heterogeneous catalytic oxidation for the degradation of p-nitrophenol in aqueous solution by persulfate activated with $CuFe_2O_4$ magnetic nano-particles, Chem. Eng. J. 324 (2017) 63–73.
[37] Y. Ji, C. Dong, D. Kong, J. Lu, Q. Zhou, Heat-activated persulfate oxidation of atrazine: Implications for remediation of groundwater contaminated by herbicides, Chem. Eng. J. 263 (2015) 45–54.
[38] J. Chen, R. Qu, X. Pan, Z. Wang, Oxidative degradation of triclosan by potassium permanganate: Kinetics, degradation products, reaction mechanism, and toxicity evaluation, Water Res. 103 (2016) 215–223.
[39] X. Zhang, M. Feng, L. Wang, R. Qu, Z. Wang, Catalytic degradation of 2-phenylbenzimidazole-5-sulfonic acid by peroxymonosulfate activated with nitrogen and sulfur co-doped CNTs-COOH loaded $CuFe_2O_4$, Chem. Eng. J. 307 (2017) 95–104.
[40] S. Sulaiman, M. Khamis, S. Nir, F. Lelario, L. Scrano, S.A. Bufo, G. Mecca, R. Karaman, Stability and removal of atorvastatin, rosuvastatin and simvastatin from wastewater, Environ. Technol. 36 (2015) 3232–3242.
[41] Y. Fan, Y. Ji, D. Kong, J. Lu, Q. Zhou, Kinetic and mechanistic investigations of the degradation of sulfamethazine in heat-activated persulfate oxidation process, J. Hazard. Mater. 300 (2015) 39–47.